Optics Communications 412 (2018) 85–89

Contents lists available at ScienceDirect

Optics Communications

journal homepage: www.elsevier.com/locate/optcom

Thermally tunable broadband terahertz metamaterials with negative refractive index

Weili Li, Qinglong Meng, Renshuai Huang, Zheqiang Zhong, Bin Zhang *

College of Electronics and Information Engineering, Sichuan University, Chengdu, 610065, China

ARTICLE INFO

Keywords:
Terahertz metamaterials
Thermally tunable
Transmission
Amplitude
Phase
Negative refractive index

ABSTRACT

A thermally tunable broadband metamaterials with negative refractive index (NRI) is investigated in terahertz (THz) region theoretically. The metamaterials is designed by fabricating two stand-up opposite L shape metallic structures on fused quartz substrate, and the indium antimonide (InSb) is filled in the bottom gap of the two L shape structures. The tunability is attributed to the InSb because the InSb can changes the capacitance of the gap area by adjusting the temperature. The transmission characteristics and the retrieved electromagnetic parameters of the metamaterials are analyzed. Results indicate that the resonant frequency and amplitude modulation of the metamaterials can be tuned continuously in broadband range (about 0.62 THz), and the phase modulation from −2 to 3 rad is also achieved within broadband range (about 0.8 THz). In addition, the metamaterials shows dual-band NRI behaviors at 0.4–0.9 THz and 1.06–1.15 THz when the temperature increases to 400 K. The wedge-shaped prism simulations are implemented to verify the NRI characteristics and indicate that the NRI of the metamaterials can be achieved.

1. Introduction

Metamaterials, composed of the subwavelength structure cells arranged in periodic arrays, are artificial materials with unnatural electromagnetic properties. They have attracted intensive attention owing to lots of promising unique and properties, such as negative refractive index [1], negative magnetic permeability [2], unnaturally high refractive index [3], extreme anisotropic [4], hyperbolic dispersion relation [5], etc. Especially, metamaterials with negative refractive index have potential applications in superlenses, subwavelength imaging, electromagnetic cloak [6–8], etc. Recently, some semiconductors have been judiciously joined into metamaterials designs to achieve dynamical control of resonant frequency, transmission amplitude, phase and even negative refractive index [9–14]. Jun Zhu et al. achieved thermal broadband tunable THz metamaterials from 0.90 THz to 1.49 THz by planar (split-ring resonators) SRRs and semiconductor InSb [9]. Padilla W J et al. achieved transmission amplitude modulation from 15% to over 70% at resonant frequency by planar SRRs and photoexcitation semiconductor Gallium Arsenide (GaAs) [11]. Cojocari M V et al. obtained not only broadband frequency modulation from 4.84 THz to 5.39 THz, but also excellent phase modulation by toroidal SRRs and semiconductor Silicon (Si) [14]. Compared to other semiconductors, the semiconductor InSb is widely used in thermally tunable devices such as terahertz filters, modulators and so on [15,16] due to its carriers concentration very sensitive to temperature. However, in previous work, the majority of metamaterials are designed with the planar structures. Therefore, the modulations of frequency, transmission amplitude or phase are accomplished by tuning the electric or the magnetic response. An optically controlled stand-up SRRs THz metamaterials with frequency and amplitude modulation has been proposed in Ref [17], unfortunately, it cannot obtain the NRI due to its large bi-anisotropy. Although Meng Q et al. proposed a hybrid THz metamaterials which is composed of planar SRRs and stand-up SRRs, and achieved the dual-band resonance response and broadband NRI by tuning the magnetic response frequency [18], the unit structure seems to be complex relatively. There is rare report on multifunctional or broadband NRI THz metamaterials accomplished by stand-up SRRs only.

In this paper, a thermally tunable broadband NRI terahertz metamaterials is presented. The metamaterials is composed of two opposite stand-up L shape metallic structures and the embedded InSb. A broadband frequency modulation from 0.45 THz to 1.07 THz can be realized by changing the temperature, and the transmission amplitude at the resonant frequency can also be tuned from 57% to 7%. Meanwhile, the phase variation of the THz wave varies from −2 to 3 rad. The bi-anisotropy of the metamaterials is also analyzed, because the metamaterials is not symmetrical with respect to the electric field vector.

---

* Corresponding author.
E-mail address: zhangbin_scu@scu.edu.cn (B. Zhang).

https://doi.org/10.1016/j.optcom.2017.11.076
Received 5 August 2017; Received in revised form 31 October 2017; Accepted 27 November 2017

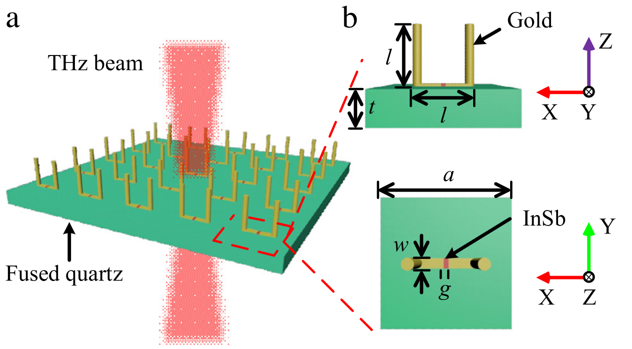

Fig. 1. (a) Schematic illustration of the proposed metamaterials and (b) structure of unit cell.

The dual-band NRI that is caused by the electromagnetic coupling effect of the metamaterial appears at 0.4–0.9 THz and 1.06–1.15 THz when the temperature increases to 400 K. The calculated transmission characteristics, the distributions of electric field and surface currents, as well as the extracted constitutive parameters are illustrated to explain the properties of the metamaterials. Furthermore, the wedge-shaped prism simulations are implemented to verify the NRI characteristics.

2. Structure of metamaterials

The unit of the metamaterials is composed of two opposite stand-up L shape metallic structures, in the middle of which is thermo-sensitive semiconductor InSb, as shown in Fig. 1. Although the unit structure is somewhat similar to that in Ref [19], their control methods and responses are obviously different. The metamaterials in Ref [19] with electromagnetically induced transparency resonance is modulated by varying the structure parameters. Here, the metamaterials with dynamic control of frequency, amplitude and phase are achieved by adjusting the temperature to control the conductivity of InSb, and the NRI has been observed as well.

As shown in Fig. 1(b), a pair of opposite stand-up L shape metallic structures are fabricated on the fused quartz substrate, between which is filled with semiconductor InSb. The parameters of the structure are as follows: a = 80 μm, w = 6 μm, g = 3 μm, t = 20 μm, l = 41 μm. The thickness of bottom metallic strip is 1.5 μm and the metallic structures are lossy gold with the electric conductivity (σ) of 7×10^6 S/m [20]. In the structure, the lossless fused quartz with the permittivity (ε) of 3.8 is chosen as dielectric substrate [19]. The THz wave is normally incident on the sample with electric field $\boldsymbol{E}$ paralleling to the $\boldsymbol{X}$ direction (The magnetic field $\boldsymbol{H}$ of THz wave propagates along with $\boldsymbol{Y}$ direction).

3. Results and discussions

In order to analyze the transmission spectra and the phase variation at different temperatures, the finite difference time domain (FDTD) has been performed by using the commercial software CST Microwave Studio. The typical simulation results are illustrated in Fig. 2.

Fig. 2(a) shows that the resonant frequency blue-shifts from 0.45 THz to 1.07 THz when the temperature increases from 250 K to 400 K. Meanwhile, the transmission amplitude t (ω) at resonant frequency decreases from 57% to 7%. In addition, broadband phase modulation phenomena are also observed in Fig. 2(b). The phase of THz wave changes from −2 to 3 rad in the frequency range from 0.4 THz to 1.2 THz when the temperature rises from 250 K to 400 K. Compared to the broadband resonance achieved by tuning the magnetic response frequency to red-shift the electric response frequency [18], the broadband frequency blue-shift and phase modulation can be achieved by a stand-up SRRs only. In order to further study the response mechanism of the proposed metamaterials, Fig. 3 shows the calculated electric field and surface current distributions at resonant frequency 0.45 THz, 0.82 THz and 1.07 THz when the corresponding temperature of InSb are 250 K, 310 K and 400 K, respectively.

As shown in Fig. 3(a), (c) and (e), the electric field distributions at the resonant frequency of 0.45 THz are firstly concentrated on gap, whereas the electric field gradually distributes on the two metallic cylinders at the resonant frequency of 0.82 THz and 1.07 THz with the increasing temperature. Correspondingly, the surface current distributions at the resonant frequency are mainly concentrated on the metallic structure and become more and more intense with the increasing temperature, as shown in Fig. 3(b), (d) and (f).

According to Fig. 3, the stand-up SRRs can be modeled as LC circuits, where the inductance arises from the two L shape metallic structures and the capacitance arises from the bottom gap region. Because the semiconductor InSb is located in the gap, the capacitance is adjustable with variation of temperature [9]. The capacitance together with the inductance from the stand-up SRRs determine the resonant frequency ω_m of the metamaterial structure, i.e., $\omega_m \propto 1/(LC)^{1/2}$ [21], which result in the shift of the resonant frequency ω_m with the temperature [9]. As a result, the resonant frequency ω_m increases with the increase of the temperature (as shown in Fig. 2(a)), because the bottom gap capacitance decreases with the increase of the temperature. Meanwhile, as shown in Fig. 3(b), (d) and (e), the resonant strength increases with the temperature. Thus, the transmission amplitude at resonant frequency decreases with the increase of the conductivity σ_{InSb}.

The constitutive parameters from full wave electromagnetic simulations are extracted to study the electromagnetic properties of the metamaterial at different temperatures [22–24]. Meanwhile, the bi-anisotropy is considered because the stand-up SRRs are not symmetric with respect to the electric field vector [25]. Fig. 5 gives the constitutive parameters retrieved from full wave electromagnetic simulations.

Fig. 4(a) shows that the real part of the refractive index is always positive. This is because both of the permittivity and permeability are not negative in the same frequency band. However, when the temperature is 400 K, the dual-band NRI is observed at 0.4–0.9 THz and 1.06–1.15 THz, as shown in Fig. 4(b). The presence of the NRI appears at 0.4–0.9 THz because the permittivity and permeability are simultaneously negative. It is worth noting that the refractive index at 1.06–1.15 THz is also negative though the permittivity and permeability are not simultaneously negative. If the condition of $\mu_1\varepsilon_2 + \mu_2\varepsilon_1 < 0$ is met ($\varepsilon = \varepsilon_1 + i\varepsilon_2$, $\mu = \mu_1 + i\mu_2$), the NRI can also be realized though the permeability and permittivity are not simultaneously negative [18,26]. Therefore, the NRI can be realized at both the frequency range of 0.4–0.9 THz and 1.06–1.15 THz. The NRI of the metamaterials also can be realized by the electromagnetic coupling effect of the stand-up SRRs only rather than the NRI achieved by planar SRRs and stand-up SRRs simultaneously [18]. Furthermore, all the transmission, permittivity, permeability and refractive index of the metamaterials vary with the change of the state of InSb by comparing Fig. 4(a), (b) and Fig. 2. Especially, the refractive index of the metamaterials changes from positive to dual-band NRI when the InSb transforms from an insulating to an almost conducting state.

4. Wedge-shaped prism simulations

To further verify the NRI characteristics of the metamaterials, we designed a wedge-shaped prism of the metamaterials to perform the Snell's refraction law by CST Microwave Studio, which obtains a direct image of the negative refraction behavior [27–30]. As shown in Fig. 5(a), the wedge-shaped structure is made of 54 individual unit cells, which are stacked in the $\boldsymbol{Z}$-axis. The cell structure dimensions are the same as the structure discussed above and the space of unit cell in the $\boldsymbol{Z}$ direction is 61 μm. 12 unit cells are used along the $\boldsymbol{X}$-axis and 7 unit cells are used along the $\boldsymbol{Z}$-axis. The refraction interface is characterized by a staircase pattern with two-unit-cell step in the $\boldsymbol{X}$-axis and one-unit-cell step in the $\boldsymbol{Z}$-axis, which can be referred to as a wedge with an angle 20.9°.